Published in final edited form as:
Invest Radiol. 2011 January ; 46(1): 41–47. doi:10.1097/RLI.0b013e3181f0213f.

Determinations of renal cortical and medullary oxygenation using BOLD Magnetic Resonance Imaging and selective diuretics

Lizette Warner, PhD[1], **James F. Glockner, MD, PhD**[2], **John Woollard**[3], **Stephen C. Textor, MD**[3], **Juan C. Romero, MD**[1,+,*], and **Lilach O. Lerman, MD PhD**[3,*]

[1]Department of Physiology and Biomedical Engineering, Mayo Clinic, Rochester, Minnesota

[2]Department of Radiology, Mayo Clinic, Rochester, Minnesota

[3]Division of Nephrology and Hypertension, Mayo Clinic, Rochester, Minnesota

Abstract

Objective—This study was undertaken to test the hypothesis that blood O_2 level dependent magnetic resonance imaging (BOLD MRI) can detect changes in cortical proximal tubule (PT) and medullary thick ascending limb of Henle (TAL) oxygenation consequent to successive administration of furosemide and acetazolamide (Az). Assessment of PT and TAL function could be useful to monitor renal disease states *in vivo*. Therefore, the adjunct use of diuretics that inhibit Na^+ reabsorption selectively in PT and TAL, Az and furosemide, respectively, may help discern tubular function by using BOLD MRI to detect changes in tissue oxygenation.

Material and Methods—BOLD MRI signal R2* (inversely related to oxygenation) and tissue oxygenation with intrarenal O_2 probes were measured in pigs that received either furosemide (0.5mg/kg) or Az (15mg/kg) alone, Az sequentially after furosemide (n=6 each, 15-minute intervals), or only saline vehicle (n=3).

Results—R2* decreased in the cortex of Az-treated and medulla of furosemide-treated kidneys, corresponding to an increase in their tissue O_2 assessed with probes. However, BOLD MRI also showed decreased cortical R2* following furosemide that was additive to the Az-induced decrease. Az administration, both alone and after furosemide, also decreased renal blood flow (−26±3.5 and −29.2±3%, respectively, $p<0.01$).

Conclusion—These results suggest that an increase in medullary and cortical tissue O_2 elicited by selective diuretics is detectable by BOLD MRI, but may be complicated by hemodynamic effects of the drugs. Therefore, the BOLD MRI signal may reflect functional changes additional to oxygenation, and needs to be interpreted cautiously.

Keywords

MRI; BOLD; kidney; renal oxygenation

CORRESPONDING AUTHOR: Lilach O. Lerman, MD PhD Division of Nephrology & Hypertension Mayo Clinic 200 First Street SW Rochester, MN, 55905 USA Phone + 1 507 284 4695; Fax + 1 507 266 9316; lerman.lilach@mayo.edu.
[+]Deceased
[*]The authors contributed equally to this study.

DISCLOSURES: None.

INTRODUCTION

Tubulointerstitial damage correlates with functional impairment of the kidney and is a final common pathway to end-stage renal disease(1,2). Evidence suggests a crucial role for tubulointerstitial hypoxia prior to structural microvascular damage in corresponding tubular segments of the nephron (3,4). Importantly, renal damage may involve proximal tubule (PT) or more distal tubule segments, and the site of injury constitutes an important determinant of the nature and timing of therapy (5–10). The ability to assess the function of individual nephron segments could shed light and assist in monitoring renal disease states.

Since sodium reabsorption constitutes a large part of the tubular workload in the PT and thick ascending limb of Henle (TAL), changes in tubular sodium reabsorption may be associated with corresponding reciprocal changes in renal oxygenation. Acetazolamide (Az), a carbonic anhydrase inhibitor, binds the active binding site on carbonic anhydrase, and has been shown to blunt PT Na^+ reabsorption and increase cortical tissue O_2 (11,12). Similarly, furosemide, which inhibits the NKCC2 transporter responsible for Na^+ reabsorption in the luminal border of the TAL, attenuates deoxyhemoglobin (dHb)(13) levels and increases medullary tissue O_2 (pO_2) tension(14). Importantly, changes in tissue oxygenation may be detectable *in vivo* because the characteristic magnetic resonance (MR) signal, R2*, is affected by dHb and has demonstrated inverse correlation with tissue O_2 (13,15), to the basis of blood oxygen level dependent (BOLD) MR imaging techniques.

BOLD MR imaging takes advantage of the paramagnetic properties of dHb to generate images whose signal intensity is a reflection of tissue O_2, representing both O_2 consumption (e.g. tubular work) and delivery (e.g. tissue perfusion) (13–16). The paramagnetic molecule, dHb, generates local magnetic field inhomogeneities leading to more rapid spin dephasing (or an increase in relaxivity R2*) (17,18). Conversely, diamagnetic oxyhemoglobin is devoid of these properties, and therefore the amount of dHb can be related to the signal intensity of R2*-weighted pulse sequences. Indeed, BOLD MR imaging has been used to detect decreases in R2* secondary to furosemide-induced increases in medullary tissue O_2 in various animal models and in humans with vascular occlusive disease (19–21). However similar non-invasive detection of changes in cortical oxygenation following Az administration have proven to be elusive(11).

BOLD MR takes advantage of the fact that the TAL, predominantly located in the renal medulla, consumes up to an estimated 40–60% of available O_2(22–24), and that inhibition of solute reabsorption by furosemide leads to a marked decrease in R2* and increase in tissue O_2(13,25). Selective blockade of the NKCC2 transporter using furosemide allows insight into medullary tissue O_2 changes in diabetes, renal arterial stenosis, and ureteral obstruction (13,26–28). Az may allow similar functional evaluation of the PT, because it alters cortical O_2 consumption by selectively blocking PT soluble transport, estimated to contribute up to 25% of total renal O_2 consumption. A practical BOLD MR protocol to test both PT (using Az) and TAL (using furosemide) functions would be very useful both experimentally and clinically.

Therefore, we undertook this study to test the hypothesis that BOLD MRI can detect changes in cortical and medullary tissue O_2 during sequential administration of diuretics in a single protocol. To test this hypothesis, we independently measured the R2* BOLD MRI signal, intrarenal tissue O_2, and renal hemodynamics in three experimental clearance periods (baseline, period 1, and period 2) involving administration of furosemide in period 1 and Az in period 2.

MATERIAL and METHODS

All animal experiments were performed with the approval of the Mayo Clinic Institutional Animal Care and Use Committee. Animals were anesthetized (telazol 5 mg/kg and xylazine 2 mg/kg) and maintained with mechanical ventilation of 1–2% isoflurane in room air. An ear vein catheter was introduced for drug and saline infusions (5 mL/min). The experiment consisted of three consecutive 15-minute clearance periods (baseline, period 1 and period 2, Figure 1). Six domestic pigs (furo+az, 49.1 ± 1.5 kg) were assigned to receive a bolus of furosemide (0.05 mg/kg, Sigma, St. Louis, MO, USA) (27), a long acting (100-minute half life) loop diuretic(29) in period 1, followed 15 minutes later by infusion of the short acting proximal diuretic (30–32) Az (15mg/kg, Sigma, St. Louis, MO, USA) (30–32) in period 2. In 3 additional control groups we replaced furosemide (s+az, n=6), Az (furo+s, n=6), or both (s+s, n=3) with saline vehicle (Figure 1). After a 15-minute baseline control period, drugs were administered at the beginning of the experimental period and measurements obtained at the end of each period (15 minutes later). Isotonic saline infusion was increased during diuretic administration by up to 10 ml/min to replace urinary fluid loss.

BOLD MRI Study

After anesthesia, the animal was positioned in the MRI scanner. MRI studies were performed on a Signa TwinSpeed EXCITE 1.5T system (GE Healthcare, Waukeshau, WI) using a multi-echo gradient echo sequence (TR/TE/Flip angle/FOV/BW/imaging matrix/thickness/NSA= 85ms/2.3–37.2 ms/40/32 cm/63.95kHz/256×256/5–7mm/1) to acquire the BOLD images. Imaging was performed at the conclusion of each 15-minute experimental period to determine R2*. Five to six axial-oblique BOLD images were acquired during suspended respiration, through the upper, mid and/or lower pole during a 26–32 second acquisition. A quadrature extremity coil was used for signal reception. For data analysis, regions of interest were traced in the cortex and medulla (Figure 2 A). The average region of interest signal intensity (SI) was plotted versus TE and fit to a single exponential function to generate a R2* (R2*=1/T2*) map according to the equation, $SI=C\ \exp^{-(TE/T2^*)}$ (20). The constant, C, was used tocompensate for contributions from instrumentation noise. Although another parameter can be added to compensate for noise effects from iron-poor species such as blood, the fitting obtained with a single exponential function using MATLAB (MATLAB version 7.0, The MathWorks, Inc., Cambridge, MA, USA) matches well with results obtained with the FuncTool (GE Healthcare) (33). A total of 6–10 (depending on level of bowel artifact) regions of interest (ROI) were placed in each medulla and cortex of both kidneys, and all ROI of each compartment averaged for both kidneys per pig. The groups were then compared for degree of response (percent signal change), because the absolute R2* value is a relative measure, which may vary with position in the MR magnet, shimming, coil position, and field inhomogeneities.

Tissue Oxygen Measurement

Five to seven days later, the same animals were similarly prepared, anesthetized and mechanically ventilated with room air and 1–2% isoflurane. A catheter was introduced into the external left jugular vein for infusion of 2% inulin bolus (40ml) followed by a continuous infusion (1 ml/min). A catheter was positioned in the left carotid artery for sampling arterial blood O_2 content and monitoring mean arterial pressure. The animal was kept warm with a warming blanket and temperature monitored with a thermoprobe.

Both ureters were exposed and cannulated through a small flank incision. The right kidney was also freed of connective tissue, and placed in a lexan kidney holder held upright by a manipulator stand for the remainder of the experiment. The kidney was surrounded by cotton wool soaked in saline and mineral oil and was kept warm by a saline drip (37 °C). An

ultrasound flow probe (T206 Flowmeter, Transonic), the accuracy of which is ±15% (34), was placed around the renal artery for measuring whole kidney blood flow. The flow probe was chosen to allow real-time continuous monitoring of RBF throughout the experimental period. Ventilation rate and tidal volume were adjusted to maintain arterial pO_2, pCO_2 and pH between 90–110mmHg, 35–50mmHg and 7.3–7.5 respectively (35).

Tissue O_2 was measured with Clark electrodes (Unisense, Aarhus, Denmark) as described previously(36). Briefly, the probes were calibrated and inserted into the right cortex and medulla by penetrating the kidney capsule to depths between 0.5–0.8 cm and 1–1.2 cm, respectively, as previously shown, and their placement subsequently verified with histological staining of cortex and medulla (Figure 2B,C) (36). Experimental periods similar to the prior MRI studies were then repeated, using identical drug and saline doses. Data were digitized in 1 sec intervals with Sensor Trace Basic v1.3 (Unisense, Aarhus, Denmark) and each probe's data averaged for the representative period.

Renal Function

Plasma and urine inulin concentrations (37,38) were measured during the invasive studies using a standard colorimetric method. Glomerular filtration rate (GFR) was estimated by the clearance of inulin as $GFR = U_{inu}*V / P_{inu}$, where U_{inu} is the urinary concentration of inulin, V is the urine flow rate (ml/min) and P_{inu} is the plasma concentration of inulin.

Statistical Analysis

Comparisons within groups were performed by repeated measure ANOVA and paired Student's *t* test. Post-hoc comparisons between groups were conducted with Tukey Kramer. Results are reported as mean ± SEM and statistical significance was accepted for $p<0.01$.

RESULTS

There were no differences in body weight, mean arterial pressure, or basal single kidney function among the groups (Table 1, ANOVA $p>0.05$).

Tissue Oxygenation Detected by BOLD MRI

Cortical and medullary R2* values detected by MRI were similar at baseline in all groups (Table 2). Serial measurements of R2* in the control (s+s) cortex and medulla showed no change from baseline throughout the two periods (Table 2). Infusion of furosemide during period 1 (in furo+s and furo+az) reduced both cortical and medullary R2* (Table 2, Figure 3), a decrease that stabilized and persisted throughout period 2. However, the decrease in medullary R2* exceeded the decrease in cortical R2* only in the furo+s group ($p=0.02$). Az administration during the 2^{nd} experimental period in s+az and furo+az groups induced a cortical R2* decrease (Figure 3A), which was greater in the group in which Az was preceded by furo (furo+az) than in the s+az group (Figure 3, $p<0.05$).

Tissue Oxygenation Detected by O_2 Probes

Cortical and medullary tissue O_2 obtained using O_2 probes were similar in all groups at baseline (Table 3). Cortical and medullary tissue O_2 in the control (s+s) group remained unchanged throughout the experiment. Administration of furo in period 1 in the furo+az and furo+s groups did not affect cortical O_2 levels (Figure 4A), while medullary tissue O_2 showed an increase that persisted during the second period (Figure 4B), in line with the long-acting diuretic effect of furosemide. Az administration during period 2 induced a significant increase in cortical tissue O_2 in the Az receiving groups (furo+az and s+az, $p<0.05$) and medullary tissue O_2 in the Az only receiving group (s+az, $p<0.05$) compared to all the other groups (Figure 4A).

Renal Hemodynamics

There were no significant changes in RBF in any group during period 1, regardless of treatment (Figure 5). RBF decreased during period 2 only in the groups that received Az (furo+az and s+az, to 200±12.4 and 221±7.6 ml/min, respectively, $p<0.001$ vs. baseline, Figure 5). GFR also decreased in period 2 in the same groups (to 25.5±3.4 and 27.0±3.6 ml/min, respectively, $p<0.05$ compared to baseline). The urinary flow rate increased during period 1 in the furosemide receiving groups, furo+az and furo+s (to 8.6±2.1 and 9.3±0.7 ml/min, $p<0.001$ vs. baseline), and in period 2 in the Az-treated groups, furo+az and s+az (to 10.3±2.6 and 6.2±1.1 ml/min, $p<0.001$ vs. baseline).

DISCUSSION

Characterizing the influence of diuretics on tissue O_2 consumption with MRI may have significant clinical implication, because such an approach may non-invasively disclose cortical and medullary function in cases in which regional function may be useful for clinical diagnosis and monitoring. The present study establishes changes in intrarenal oxygenation using MRI and O_2 microelectrodes during administration of furosemide and acetazolamide, alone or sequentially, to distinguish proximal and TAL function. We observed that sequential characterization of two different nephron segments with BOLD-MRI is feasible but limited by effects of acetazolamide and furosemide on renal functional attributes other than oxygen consumption.

Recent evidence indicates that cortical tissue O_2 rises after administration of acetazolamide alone(12,39), and that medullary tissue O_2 elevates with furosemide alone(12). These characteristics may be useful for studying tubular function in the cortex or medulla, because a large part of renal O_2 consumption is derived from tubular work. Moreover, these might be detectable *in vivo* because the characteristic MR signal, R2*, has demonstrated inverse correlation with tissue oxygenation (28,40) and is a valuable non-invasive imaging technique capable of assessing renal medullary function in healthy humans and in disease (41–44). However, a comparable cortical functional test, which could also benefit clinical diagnosis and treatment, remains elusive in part due to difficulty in detecting changes in cortical oxygenation following Az administration(13). In particular, the ability to probe segmental nephron function in one sequence could allow monitoring it in a practical manner. We therefore tested the hypothesis that using selective diuretics that inhibit proximal tubular or TAL transport might be useful for discerning cortical and medullary tubular function in vivo.

As previously reported (27,38,45), we observed that, likely via inhibition of Na^+ reabsorption in the TAL, furosemide caused a measurable increase in medullary oxygenation detected as a decrease in BOLD-MRI R2* and an increase in O_2 levels assessed with probes. On the other hand, BOLD-MRI, but not O_2 microelectrodes, demonstrated an increase in cortical tissue oxygenation elicited by furosemide. The discrepancy between BOLD-MRI and O_2 microelectrodes could stem from several factors. Firstly, furosemide might have a direct (albeit subtle) effect on cortical signals, as it inhibits some isoforms of carbonic anhydrase (46). This might be magnified by the decrease in medullary oxygen consumption that returns more oxygenated blood to the cortex, which might not be detectable in the limited sampling volume of O_2 microelectrodes. In addition, although R2 changes were not specifically measured in the present study, a prominent R2 effect in the cortex associated with fluid volume shifts may have also contributed to the R2* changes observed during furosemide. We also cannot exclude partial volume averaging with medullary tissue during selection of the cortical ROI. Furthermore, the BOLD signal is affected not only by O_2 consumption, but also by perfusion (13), the impact of which is difficult to assess without direct measurements of regional renal perfusion. Cortical

perfusion is up to ten times that of the medulla (39), and although furosemide did not induce a measurable change in RBF, local redistribution of flow, O_2 consumption, or capillary recruitment, might also have contributed to the discrepancy between BOLD-MRI and O_2 probes. Indeed, the relationship among tissue perfusion, O_2 consumption, and oxygenation warrants further investigation as they may all affect the R2* signal detected with BOLD-MRI.

In contrast to furosemide, acetazolamide induced a preferential increase in cortical tissue oxygenation that was detected by both methods and potentiated by furosemide. Indeed, the present study demonstrates that sequential administration of furosemide followed by acetazolamide produces a reduction in both medullary and cortical BOLD MRI R2* that was coupled to an increase in medullary and cortical oxygenation detected by tissue O_2 probes, which was not observed in a prior study using acetazolamide(13). Importantly, Az reduces tubular workload by inhibiting PT transport, thereby increasing tissue O_2 (resulting in a reduced R2*). On the other hand, acetazolamide also elicited a concomitant reduction in RBF, an effect known to decrease O_2 delivery and renal oxygenation (36,47–49) that should thus counteract the decrease in O_2 consumption achieved by inhibition of proximal tubular transport. Az has been suggested to reduce RBF due to afferent vasoconstriction and may significantly alter tubular dynamics because of intrinsic vasoactive factors and tubulo-glomerular feedback (27,36,50,51). A decrease in GFR by similar mechanisms may also serve to decrease renal O_2 consumption. In this study, the reduction in O_2 demand likely outweighed the effect of the diminished blood supply, as evidenced by overall elevated tissue O_2 and reduced R2*. Interestingly, medullary tissue O_2 was maintained despite reduced RBF in the Az treated groups. Az might have redistributed intra-renal perfusion towards the medulla, although we cannot rule out the possibility that it also decreased medullary O_2 consumption by nonspecific mechanisms. The hemodynamic and renal functional effects of Az might therefore hamper interpretation of changes in regional perfusion, oxygenation, and the BOLD MRI signal. Nevertheless, our observations suggest that BOLD MRI is capable of detecting both increases in cortical and medullary O_2 in normal kidneys using a single protocol with two different diuretics.

Recently, anatomic corticomedullary differentiation has been used to characterize structural distinction of the cortex from the medulla on T1 weighted MRI images, and may become a promising technique in diagnosing specific pathology in renal disease(52). Functional corticomedullary differentiation assessed using BOLD MRI, which relies on changes in intra-renal concentrations of dHb (13,28), can also be valuable for detecting renal pathology. Nonetheless, this technique faces several challenges. The BOLD MRI technique is suitable for low oxygen tension environments, in which the O_2 hemoglobin dissociation curve has maximal effect, and may be limited by sensitivity to changes in perfusion and O_2 consumption (13). The hemodynamic effects of Az may diminish its application with BOLD MRI for assessing changes in cortical oxygenation. Additionally, the change in cortical R2* following Az was less pronounced than the medullary response to furosemide. We used Az at doses similar to those used in previous studies. Since higher doses of Az have not elicited greater responses(30–32), and low doses of Az have been shown to be as effective as higher doses responses(53), the limited R2* response to Az is likely not attributable to sub-optimal dosing. Nevertheless, the technique is versatile and merits further evaluation of alternative diuretics devoid of hemodynamic alterations and more selective inhibitors of PT consumption, such as specific inhibitors of the cytosolic carbonic anhydrase isozyme, CAII, which serves as a more specific indicator of proximal O_2 consumption(54).

Our findings are consistent with studies showing increased renal O_2 tension with carbonic anhydrase inhibitors(12), although previous MRI studies detected no change in tissue oxygenation following Az alone(13) in humans. The order for diuretic administration was

therefore chosen to inhibit first the TAL and then the proximal nephron, to prevent Az from increasing medullary oxygen demand by elevating distal tubule delivery and workload. Importantly, because of its short half life (30–32), we employed a continuous infusion of Az while simultaneously monitoring hemodynamic effects. As previously shown (55,56), Az elicited a sustained decrease in RBF, which might be secondary to a direct effect of this agent on the renal circulation (55) and was not likely due to volume depletion, since saline infusion was increased to counterbalance urinary volume loss. Future studies will benefit from including measurements of regional perfusion to test the possibility that Az induced local changes that impacted regional tissue oxygenation. In addition, we compared regional BOLD-MRI measurements to those obtained with Clark type O_2 electrodes in the attempt to measure oxygen consumption by diuretics known for their metabolic affects. Although the Clark type O_2 electrodes are fragile, consume a small fraction of O_2 at the tip of the electrode (57) and require penetration of the kidney capsule, they are considered reference standard for assessing tissue O_2. The advent of probes that can both detect oxygen content and regional blood flow, and of dynamic fluorescence quenching that offers a flexible MR compatible probe (58,59), may be more useful tools in the future.

Conclusions

The present study demonstrates that BOLD-MRI can detect increases in medullary oxygenation with furosemide and cortical oxygenation with acetazolamide, either individually or sequentially. Alas, we found that furosemide also increased cortical oxygenation as assessed by BOLD-MRI (but not by O_2 electrodes) in a manner that was additive to Az, and possibly secondary to hemodynamic effects. In addition, the increase in cortical oxygenation elicited by Az alone (detected by both techniques) was modest, possibly due to a concurrent decline in RBF. Our results therefore support the notion that the BOLD MRI R2* signal reflects changes other than tissue oxygenation alone. These observations in swine may have clinical relevance because the pig kidney is anatomically and physiologically comparable to the human kidney, where the BOLD MRI technique has already been employed. Application of BOLD MRI in conjunction with diuretics that have specific sites of actions along the nephron may be useful to explore alterations in renal tissue oxygen consumption and tubular function. However, further studies are needed to determine the interaction between renal hemodynamics, perfusion, tubular workload, and oxygenation in order to better interpret changes in R2*.

Acknowledgments

Supported in part by NIH grants HL085307, DK73608, HL77131, DK73013, HL16496, 1F31HL094060, and by the American Physiological Society Porter Fellowship. This work is dedicated to our inspiring mentor, the late Dr. J. Carlos Romero.

References

1. Nath KA. Tubulointerstitial changes as a major determinant in the progression of renal damage. Am J Kidney Dis 1992;20:1–17. [PubMed: 1621674]
2. Anderson S. Mechanisms of injury in progressive renal disease. Exp Nephrol 1996;4(Suppl 1):34–40. [PubMed: 9001895]
3. Nangaku M. Chronic Hypoxia and Tubulointerstitial Injury: A Final Common Pathway to End-Stage Renal Failure. J Am Soc Nephrol 2006;17:17–25. [PubMed: 16291837]
4. Fine LG, Orphanides C, Norman JT. Progressive renal disease: the chronic hypoxia hypothesis. Kidney Int 1998;65(Suppl):S74–78.
5. Andreoli SP. Acute renal failure. Curr Opin Pediatr 2002;14:183–188. [PubMed: 11981288]
6. Alfonzo AV, Fox JG, Imrie CW, Roditi G, Young B. Acute renal cortical necrosis in a series of young men with severe acute pancreatitis. Clin Nephrol 2006;66:223–231. [PubMed: 17063988]

7. Batuman V. Proximal tubular injury in myeloma. Contrib Nephrol 2007;153:87–104. [PubMed: 17075225]
8. Suresh M, Laboi P, Mamtora H, Kalra PA. Relationship of renal dysfunction to proximal arterial disease severity in atherosclerotic renovascular disease. Nephrol Dial Transplant 2000;15:631–636. [PubMed: 10809803]
9. Rossi C, Boss A, Artunc F, et al. Comprehensive assessment of renal function and vessel morphology in potential living kidney donors: an MRI-based approach. Invest Radiol 2009;44:705–711. [PubMed: 19809340]
10. Sadick M, Schock D, Kraenzlin B, Gretz N, Schoenberg SO, Michaely HJ. Morphologic and dynamic renal imaging with assessment of glomerular filtration rate in a pcy-mouse model using a clinical 3.0 Tesla scanner. Invest Radiol 2009;44:469–475. [PubMed: 19465861]
11. Brezis M, Rosen S, Silva P, Epstein FH. Selective vulnerability of the medullary thick ascending limb to anoxia in the isolated perfused rat kidney. J Clin Invest 1984;73:182–190. [PubMed: 6690477]
12. Brezis M, Agmon Y, Epstein FH. Determinants of intrarenal oxygenation. I. Effects of diuretics. Am J Physiol Renal Physiol 1994;267:F1059–1062.
13. Prasad PV, Edelman RR, Epstein FH. Noninvasive Evaluation of Intrarenal Oxygenation With BOLD MRI. Circulation 1996;94:3271–3275. [PubMed: 8989140]
14. Baudelet C, Gallez B. How does blood oxygen level-dependent (BOLD) contrast correlate with oxygen partial pressure (pO2) inside tumors? Magn Reson Med 2002;48:980–986. [PubMed: 12465107]
15. Yamamoto T, Kato T. Paradoxical correlation between signal in functional magnetic resonance imaging and deoxygenated haemoglobin content in capillaries: a new theoretical explanation. Phys Med Biol 2002;47:1121–1141. [PubMed: 11996059]
16. Li LP, Ji L, Santos EA, Dunkle E, Pierchala L, Prasad P. Effect of nitric oxide synthase inhibition on intrarenal oxygenation as evaluated by blood oxygenation level-dependent magnetic resonance imaging. Invest Radiol 2009;44:67–73. [PubMed: 19034027]
17. Duyn JH, Moonen CT, van Yperen GH, de Boer RW, Luyten PR. Inflow versus deoxyhemoglobin effects in BOLD functional MRI using gradient echoes at 1.5 T. NMR Biomed 1994;7:83–88. [PubMed: 8068530]
18. Ogawa S, Lee TM, Kay AR, Tank DW. Brain magnetic resonance imaging with contrast dependent on blood oxygenation. Proc Natl Acad Sci U S A 1990;87:9868–9872. [PubMed: 2124706]
19. Li LP, Ji L, Lindsay S, Prasad PV. Evaluation of intrarenal oxygenation in mice by BOLD MRI on a 3.0T human whole-body scanner. J Magn Reson Imaging 2007;25:635–638. [PubMed: 17279536]
20. Textor SC, Glockner JF, Lerman LO, et al. The Use of Magnetic Resonance to Evaluate Tissue Oxygenation in Renal Artery Stenosis. J Am Soc Nephrol 2008;19:780–788. [PubMed: 18287564]
21. Alford SK, Sadowski EA, Unal O, et al. Detection of acute renal ischemia in swine using blood oxygen level-dependent magnetic resonance imaging. J Magn Reson Imaging 2005;22:347–353. [PubMed: 16104014]
22. Sejersted OM, Mathisen O, Kiil F. Oxygen requirement of renal Na-K-ATPase-dependent sodium reabsorption. Am J Physiol Renal Physiol 1977;232:F152–158.
23. Kiil F, Aukland K, Refsum HE. Renal sodium transport and oxygen consumption. Am J Physiol 1961;201:511–516. [PubMed: 13755902]
24. Chamberlin ME, LeFurgey A, Mandel LJ. Suspension of medullary thick ascending limb tubules from the rabbit kidney. Am J Physiol 1984;247:F955–964. [PubMed: 6095684]
25. Gloviczki ML, Glockner J, Gomez SI, et al. Comparison of 1.5 and 3 T BOLD MR to study oxygenation of kidney cortex and medulla in human renovascular disease. Invest Radiol 2009;44:566–571. [PubMed: 19668000]
26. Sara K, Alford EAS, Orhan Unal Jason A, Polzin Daniel W, Consigny Frank R, Korosec Thomas M, Grist. Detection of acute renal ischemia in swine using blood oxygen level-dependent magnetic resonance imaging. Journal of Magnetic Resonance Imaging 2005;22:347–353. [PubMed: 16104014]

27. Juillard L, Lerman LO, Kruger DG, et al. Blood oxygen level-dependent measurement of acute intra-renal ischemia. Kidney Int 2004;65:944–950. [PubMed: 14871414]
28. Pedersen M, Dissing TH, Morkenborg J, et al. Validation of quantitative BOLD MRI measurements in kidney: Application to unilateral ureteral obstruction. Kidney Int 2005;67:2305–2312. [PubMed: 15882272]
29. Brater DC. Clinical pharmacology of loop diuretics. Drugs 1991;41(Suppl 3):14–22. [PubMed: 1712712]
30. DuBose TD Jr. Lucci MS. Effect of carbonic anhydrase inhibition on superficial and deep nephron bicarbonate reabsorption in the rat. J Clin Invest 1983;71:55–65. [PubMed: 6848559]
31. Knox FG, Haas JA, Lechene CP. Effect of parathyroid hormone on phosphate reabsorption in the presence of acetazolamide. Kidney Int 1976;10:216–220. [PubMed: 787619]
32. Brater DC, Kaojarern S, Chennavasin P. Pharmacodynamics of the diuretic effects of aminophylline and acetazolamide alone and combined with furosemide in normal subjects. J Pharmacol Exp Ther 1983;227:92–97. [PubMed: 6620175]
33. Sadowski EA, Fain SB, Alford SK, et al. Assessment of acute renal transplant rejection with blood oxygen level-dependent MR imaging: initial experience. Radiology 2005;236:911–919. [PubMed: 16118170]
34. Lerman LO, Schwartz RS, Grande JP, Sheedy PF, Romero JC. Noninvasive evaluation of a novel swine model of renal artery stenosis. J Am Soc Nephrol 1999;10:1455–1465. [PubMed: 10405201]
35. Tobin MJ. Mechanical ventilation. N Engl J Med 1994;330:1056–1061. [PubMed: 8080509]
36. Warner L, Gomez SI, Bolterman RJ, et al. Regional decreases in renal oxygenation during graded acute renal arterial stenosis: a case for renal ischemia. Am J Physiol Regul Integr Comp Physiol 2009;296:R67–71. [PubMed: 18971350]
37. Krier JD, Ritman EL, Bajzer Z, Romero JC, Lerman A, Lerman LO. Noninvasive measurement of concurrent single-kidney perfusion, glomerular filtration, and tubular function. Am J Physiol Renal Physiol 2001;281:F630–638. [PubMed: 11553509]
38. Gomez SI, Warner L, Haas JA, et al. Increased hypoxia and reduced renal tubular response to furosemide detected by BOLD magnetic resonance imaging in swine renovascular hypertension. Am J Physiol Renal Physiol 2009;297:F981–986. [PubMed: 19640896]
39. Epstein FH. Renal Metabolism. Kidney Int 1997;51:381–385. [PubMed: 9027710]
40. Li LP, Storey P, Pierchala L, Li W, Polzin J, Prasad P. Evaluation of the reproducibility of intrarenal R2* and DeltaR2* measurements following administration of furosemide and during waterload. J Magn Reson Imaging 2004;19:610–616. [PubMed: 15112311]
41. Schachinger H, Klarhofer M, Linder L, Drewe J, Scheffler K. Angiotensin II Decreases the Renal MRI Blood Oxygenation Level-Dependent Signal. Hypertension 2006;47:1062–1066. [PubMed: 16618841]
42. Djamali A, Sadowski EA, Muehrer RJ, et al. BOLD-MRI assessment of intrarenal oxygenation and oxidative stress in patients with chronic kidney allograft dysfunction. Am J Physiol Renal Physiol 2007;292:F513–522. [PubMed: 17062846]
43. Epstein FH, Veves A, Prasad PV. Effect of diabetes on renal medullary oxygenation during water diuresis. Diabetes Care 2002;25:575–578. [PubMed: 11874950]
44. Han F, Xiao W, Xu Y, et al. The significance of BOLD MRI in differentiation between renal transplant rejection and acute tubular necrosis. Nephrol Dial Transplant. 2008
45. Textor SC. Revascularization in atherosclerotic renal artery disease. Kidney Int 1998;53:799–811. [PubMed: 9507232]
46. Temperini C, Cecchi A, Scozzafava A, Supuran CT. Carbonic anhydrase inhibitors. Comparison of chlorthalidone, indapamide, trichloromethiazide, and furosemide X-ray crystal structures in adducts with isozyme II, when several water molecules make the difference. Bioorg Med Chem 2009;17:1214–1221. [PubMed: 19119014]
47. Yoshida M, Soejima H, Ueda S, K I. Role of renal prostaglandin E2 in two-kidney, one-clip renovascular hypertension in rabbits. Nephron 1986;44:142–149. [PubMed: 3534609]

48. Just A, Arendshorst WJ. Dynamics and contribution of mechanisms mediating renal blood flow autoregulation. Am J Physiol Regul Integr Comp Physiol 2003;285:R619–631. [PubMed: 12791588]
49. Zhou X, Kost CK Jr. Adenosine A1 Receptor Antagonist Blunts Urinary Potassium Excretion, but Not Renal Hemodynamic Effects, Induced by Carbonic Anhydrase Inhibitor in Rats. J Pharmacol Exp Ther 2006;316:530–538. [PubMed: 16278313]
50. Leyssac PP, Karlsen FM, Skott O. Dynamics of intrarenal pressures and glomerular filtration rate after acetazolamide. Am J Physiol 1991;261:F169–178. [PubMed: 1858899]
51. Tucker BJ, Steiner RW, Gushwa LC, Blantz RC. Studies on the tubulo-glomerular feedback system in the rat. The mechanism of reduction in filtration rate with benzolamide. J Clin Invest 1978;62:993–1004. [PubMed: 711863]
52. Lee VS, Kaur M, Bokacheva L, et al. What causes diminished corticomedullary differentiation in renal insufficiency? J Magn Res Imag 2007;25:790–795.
53. Friedland BR, Mallonee J, Anderson DR. Short-Term Dose Response Characteristics of Acetazolamide in Man. Arch Ophthalmol 1977;95:1809–1812. [PubMed: 334132]
54. Scozzafava A, Briganti F, Ilies MA, Supuran CT. Carbonic Anhydrase Inhibitors: Synthesis of Membrane-Impermeant Low Molecular Weight Sulfonamides Possessing in Vivo Selectivity for the Membrane-Bound versus Cytosolic Isozymes1. J. Med. Chem 2000;43:292–300. [PubMed: 10649985]
55. Yeyati NL, Altenberg GA, Adrogue HJ. Mechanism of acetazolamide-induced rise in renal vascular resistance assessed in the dog whole kidney. Ren Physiol Biochem 1992;15:99–105. [PubMed: 1375769]
56. Zhou X, Kost CK Jr. Adenosine A1 receptor antagonist blunts urinary potassium excretion, but not renal hemodynamic effects, induced by carbonic anhydrase inhibitor in rats. J Pharmacol Exp Ther 2006;316:530–538. [PubMed: 16278313]
57. Leong C-L, Anderson WP, O'Connor PM, Evans RG. Evidence that renal arterial-venous oxygen shunting contributes to dynamic regulation of renal oxygenation. Am J Physiol Renal Physiol 2007;292:F1726–1733. [PubMed: 17327497]
58. O'Connor PM, Kett MM, Anderson WP, Evans RG. Renal medullary tissue oxygenation is dependent on both cortical and medullary blood flow. Am J Physiol Renal Physiol 2006;290:F688–694. [PubMed: 16219913]
59. Jensen AM, Norregaard R, Topcu SO, Frokiaer J, Pedersen M. Oxygen tension correlates with regional blood flow in obstructed rat kidney. J Exp Biol 2009;212:3156–3163. [PubMed: 19749109]

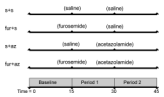

Figure 1.

Schematic of the experimental design, consisting of two experimental periods following a baseline period. Furosemide was administered in period 1 to furosemide (furo) treated groups, acetazolamide (az) was administered in period 2 and control groups were administered saline (s) in place of either or both furosemide or acetazolamide.

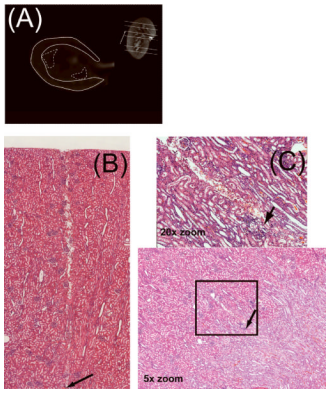

Figure 2.

Coronal image (A) with slice locations indicated with solid lines, the inset axial-oblique image distinguishes cortex (solid line) and medulla (dashed line) regions of interest (ROI). Histological staining with hematoxylin and eosin (×5) showing the path and insertion point of the probe in the cortex (B) and medulla, with inset 20× zoom (C).

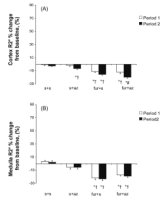

Figure 3.
Change from baseline in R2* in the cortex (A) and medulla (B) of experimental groups that received either saline (s) vehicle (s+s and s+az) or furosemide (furo) (furo+s and furo+az) in period 1, and vehicle (s+s and furo+s) or acetazolamide (az) (s+az and furo+az) in period 2. * $p<0.05$ vs. baseline, † $p<0.05$ vs. s+s , # $p<0.05$ vs. s+az in period 2.

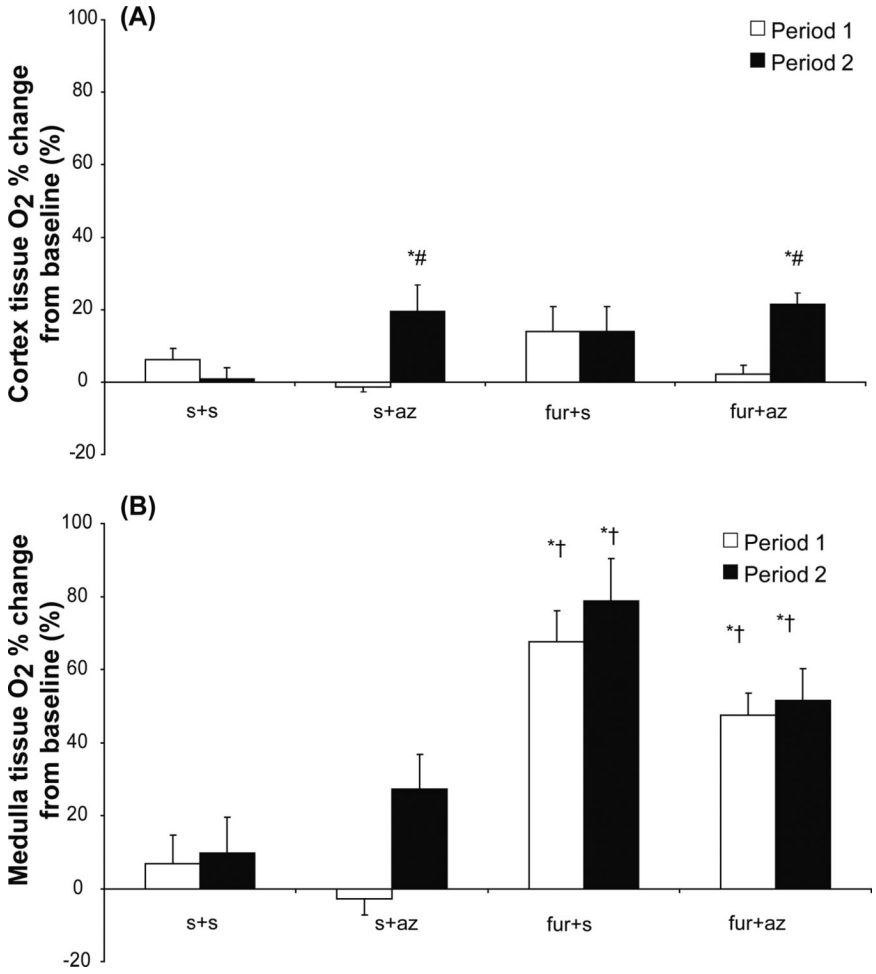

Figure 4.

Change from baseline in tissue O_2 in the renal cortex (A) and medulla (B) of experimental groups that received either saline (s) vehicle (s+s and s+az) or furosemide (furo) (furo+s and furo+az) in period 1, and vehicle (s+s and furo+s) or acetazolamide (az) (s+az and furo+az) in period 2.

* $p<0.05$ vs. baseline, † $p<0.05$ vs. s+s and s+az, # $p<0.05$ vs. s+s and furo+s.

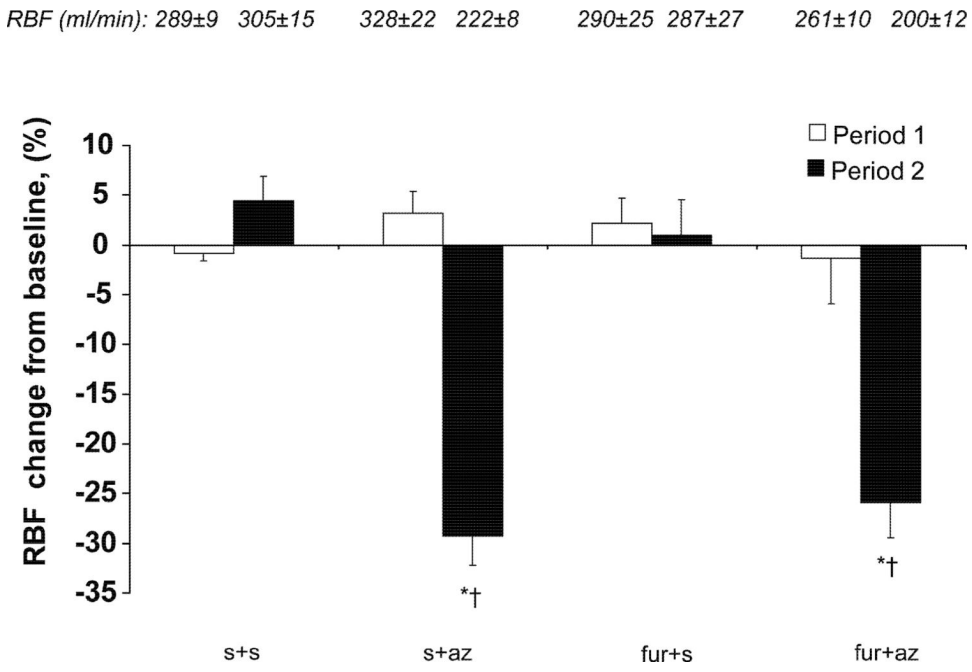

Figure 5.

Change from baseline in renal blood flow (RBF) during administration of saline (s), furosemide (furo), and/or acetazolamide (az). Experimental groups that received az showed a decrease in RBF.

*p<0.05 vs. baseline, † p<0.05 vs. s+s and furo+s

Table 1

Basal systemic and hemodynamic characteristics in the experimental groups.

Group	s+s	s+az	furo+s	furo+az
Body weight (kg)	51.1±1.3	47±2.1	48.2±1.2	49.1±1.5
MAP (mmHg)	96±4.5	94.8±3.3	94±3.7	90.1±2.7
RBF (ml/min)	292±10.5	305±22.6	284±23.4	268±7.9
GFR (ml/min)	41.7±1.3	51.8±1	47.2±5.6	48.0±4.0
Urinary flow (ml/min)	0.64±0.1	0.84±0.2	1.5±0.6	0.6±0.1

s: saline, az: acetazolamide, furo: furosemide, MAP: mean arterial pressure, RBF: single kidney renal blood flow, GFR: single kidney glomerular filtration rate

Table 2

Renal cortical and medullary BOLD MRI R2* (Hz, 1/sec) at baseline, and following administration of saline vehicle (s), acetazolamide (az), and/or furosemide (furo) in each experimental period.

Group	Cortex			Medulla		
	Baseline	Period 1	Period 2	Baseline	Period 1	Period 2
s+s	12.4 ±.8	12.2 ± .4	11.8 ± .5	15.4 ± 1.6	15.7 ± 1.5	15.5 ± 1.7
s+az	12.1 ± .3	11.6 ± .1	10.2 ± .1*#	14.6 ± 0.5	13.9 ± 0.4	14.0 ± 0.5
furo+s	12.4 ± .2	10.9 ± .3*	10.2 ± .1*	14.5 ± 0.4	11.3 ± 0.3*†#	10.9 ± 0.4*†#
furo+az	13.3 ± .2	11.7 ± .2*	10.6 ± .1*#	16.8 ± 0.6	13.0 ± .7*	12.6 ± 0.9*

*p<0.001 vs. baseline

†p<0.001 vs. s+az

#p<0.001 vs. s+s.

Table 3

Renal basal cortical and medullary tissue oxygenation, pO_2 (mmHg) determined using intra-renal O_2 probes at baseline and following administration of saline (s), acetazolamide (az), and/or furosemide (furo) in each experimental period.

	Cortex			Medulla		
	Baseline	**Period 1**	**Period 2**	**Baseline**	**Period 1**	**Period 2**
s+s	44.1 ± 1.8	46.4 ± 2.1	44.3 ± 1.3	23.5 ± 0.9	25.1 ± 2.0	25.8 ± 2.6
s+az	45.4 ± 2.4	44.7 ± 2.2	53.5 ± 1.6*†	24±1.4	23.1 ± 0.9	30.3 ± 2.5
furo+s	45.6± 1.6	50.2 ± 1.2	50.1 ± 1.3	23.5±0.9	38.5 ± 1.1*	40.8 ± 0.8*
furo+az	47.2±0.8	48.3 ± 0.9	57.3 ± 0.7*†	26.8±1.1	39.4 ±1.7*	40.6 ±2.6*

s: saline, az: acetazolamide, furo: furosemide

*p<0.01 vs. baseline pO_2

†p<0.01 vs. period 1